Biodegradable Click Capsules with Engineered Drug-Loaded Multilayers

Christopher J. Ochs, Georgina K. Such, Yan Yan, Martin P. van Koeverden, and Frank Caruso*

Centre for Nanoscience and Nanotechnology, Department of Chemical and Biomolecular Engineering, The University of Melbourne, Parkville, Victoria 3010, Australia

The design of novel polymer carriers is of high importance for a range of biomedical applications, including gene therapy,[1] drug delivery,[2−4] and microreactors.[5,6] The layer-by-layer (LbL) approach has proven to be a useful technique for the assembly of nanoengineered polymeric capsules with defined properties. LbL capsules can be assembled by exploiting various interactions, including electrostatics,[7] hydrogen bonding,[8] DNA hybridization,[9] or covalent stabilization.[10−13] For example, single-component capsules have been constructed via hydrogen bonding between poly(N-vinyl pyrrolidone) (PVPON) and poly(methacrylic acid), followed by subsequent cross-linking and PVPON removal.[14,15] Films assembled using covalent interactions have been shown to exhibit increased stability under varying conditions,[16,17] and various approaches have been used, including chemical,[18−20] photochemical,[21] electrochemical,[22] and thermal cross-linking.[23] The formation of covalently stabilized multilayer films using a combination of click chemistry and LbL assembly has proven to be a highly versatile approach.[24,25] The applicability of this approach to a wide range of materials, including low and like-charged polymers, affords single-component multilayer films and capsules.[10,26] Furthermore, click reactions, such as the widely used copper(I)-catalyzed 1,3-dipolar cycloaddition between azides and alkynes,[27,28] can be carried out under benign conditions (room temperature, water as solvent). Hence, the click−LbL approach has been extended to biologically relevant molecules and biodegradable materials, allowing for the attachment of click-functionalized peptides[29,30] and the assembly of single-component biodegradable films.[11,13]

LbL-assembled polymer capsules fulfill many criteria required for carrier systems aimed at (targeted) drug delivery. The capsules can be loaded with biologically active cargo,[31,32] degraded via various mechanisms,[33−36] and engineered with low-fouling properties.[11,37−39] The low-fouling properties are important for ultimately avoiding the aggregation and premature clearance of the capsules from the bloodstream by macrophages.[40] The attachment of targeting ligands has been shown to enhance specific capsule uptake,[41] and cargo release in response to external stimuli (e.g., near-infrared light, change of pH or ionic strength, etc.) has been demonstrated.[42,43]

ABSTRACT We report the modular assembly of a polymer−drug conjugate into covalently stabilized, responsive, biodegradable, and drug-loaded capsules with control over drug dose and position in the multilayer film. The cancer therapeutic, doxorubicin hydrochloride (DOX), was conjugated to alkyne-functionalized poly(L-glutamic acid) (PGA_{Alk}) via amide bond formation. PGA_{Alk} and $PGA_{Alk+DOX}$ were assembled via hydrogen bonding with poly(N-vinyl pyrrolidone) (PVPON) on planar and colloidal silica templates. The films were subsequently covalently stabilized using diazide cross-linkers, and PVPON was released from the multilayers by altering the solution pH to disrupt hydrogen bonding. After removal of the sacrificial template, single-component PGA_{Alk} capsules were obtained and analyzed by optical microscopy, transmission electron microscopy, and atomic force microscopy. The PGA_{Alk} capsules were stable in the pH range between 2 and 11 and exhibited reversible swelling/shrinking behavior. $PGA_{Alk+DOX}$ was assembled to form drug-loaded polymer capsules with control over drug dose and position in the multilayer system (e.g., DOX in every layer or exclusively in layer 3). The drug-loaded capsules could be degraded enzymatically, resulting in the sustained release of active DOX over ~2 h. Cellular uptake studies demonstrate that the viability of cells incubated with DOX-loaded PGA_{Alk} capsules significantly decreased. The general applicability of this modular approach, in terms of incorporation of polymer−drug conjugates in other click multilayer systems, was also demonstrated. Biodegradable click capsules with drug-loaded multilayers are promising candidates as carrier systems for biomedical applications.

KEYWORDS: click chemistry · poly(L-glutamic acid) · layer-by-layer · polymer−drug conjugate · doxorubicin

© 2010 American Chemical Society

However, the delivery and controlled release of chemotherapeutics remains a challenge, mainly due to leakage of the small cytotoxic cargo (usually $M_w < 5$ kDa) from the inherently permeable LbL carrier systems.[44,45] Recent approaches include the delivery of small hydrophobic cargo in the liposomal subcompartments of capsosomes[46] or the release of hydrophobic cargo from drug-loaded micelles assembled into planar degradable LbL multilayer films.[47,48]

The cancer therapeutic, doxorubicin hydrochloride (DOX), is a potent and well-studied DNA intercalating agent. DOX exhibits inherent fluorescence that allows direct monitoring of the intracellular fate of DOX-loaded capsules. Successful approaches for charge-driven loading of DOX to polyelectrolyte capsules rely on electrostatic interaction between the cationic DOX and an anionic (polymeric) reservoir in the capsule core.[49,50] However, in these studies, the release was triggered by displacement of DOX with salt, which may have limitations for applications under physiological conditions. More recent approaches involve the delivery of DOX from polymer-encapsulated emulsions,[51] dendrimers,[52−54] or covalent attachment of the drug to a polymeric carrier material.[55] Frechet *et al.*[52−54] reported the incorporation of enzyme- or hydrolysis-cleavable linkages for more efficient drug release from dendrimer−DOX delivery systems, while Schneider *et al.*[55] reported the assembly of multifunctional DOX-loaded nanoparticles based on a terpolymer containing 2% of a monomer to which DOX was attached through an enzymatically cleavable oligopeptide spacer. In the current work, we introduce a novel approach for the controlled assembly of DOX-loaded poly(L-glutamic acid) (PGA) capsules using a polymer−drug conjugate that allows control over drug position and dose within LbL-assembled polymeric carrier capsules.

Poly(L-glutamic acid) (PGA) is a biodegradable and biocompatible polypeptide[56,57] that contains a terminal carboxylic acid in the repeating unit, which can be used for chemical modification pre- or post-assembly. High susceptibility to degradation by lysosomal enzymes[58,59] into (natural) monomeric L-glutamic acid and non-immunogenicity *in vivo*[60] make PGA an ideal material for biomedical applications. Xyotax, an enzymatically degradable PGA−Paclitaxel conjugate,[61,62] possesses both higher solubility and improved antitumoral activity as compared to the hydrophobic parent drug. Biodegradable magnetic resonance imaging contrast agents based on PGA have also been developed.[63] However, so far, only a few attempts have been made to assemble PGA into covalently stabilized capsules. These include strategies based on electrostatic assembly with polycations such as poly(L-lysine) (PLL), resulting in interdiffusing multicomponent films that were subsequently chemically cross-linked with 1-Ethyl-3-(3-dimethylaminopropyl)carbodiimide (EDC)

chemistry.[64,65] Recently, we reported the synthesis of PGA$_{DOX}$ capsules from solid core/mesoporous shell (SCMS) silica particle templates through infiltration of the low molecular weight conjugate into the SCMS particles and subsequent cross-linking with cystamine.[66] Similarly, bioresponsive DOX-loaded poly(ethylene glycol) (PEG) spheres were synthesized from mesoporous silica particles.[67] However, both strategies[66,67] lack the fine control of the LbL approach in terms of positioning the drug within layered structures, an aspect which is important for controlling drug release.

Herein we demonstrate a versatile hydrogen bonding based approach for the assembly of click-modified PGA with PVPON on planar and colloidal templates of various sizes. To our knowledge, this is the first report utilizing the hydrogen bonding capability and the assembly of PGA with PVPON in a nanostructured film. Films constructed using biodegradable materials such as PGA are expected to have an impact on the development of biomaterials and biodegradable coatings. The films were subsequently covalently stabilized with a bisazide cross-linker, after which the PVPON was removed from the multilayer system by altering the solution pH to yield single-component PGA capsules. The pH-responsive behavior of the PGA$_{Alk}$ capsules in the range of pH 2 to 11 and the degradation of PGA$_{Alk}$ click films was studied. We also report the synthesis of a novel polymer−drug conjugate (PGA$_{Alk+DOX}$), which is then assembled into drug-loaded capsules with control over drug dose and position. The degradation profile of DOX-loaded PGA$_{Alk}$ capsules was investigated. The covalent binding of DOX to the polymer carrier allowed for controlled degradation-driven release of the drug after incubation with cells. As shown in Scheme 1, using only PGA$_{Alk}$, biodegradable capsules were assembled. More importantly, in combination with PGA$_{Alk+DOX}$, a novel biodegradable polymer−drug conjugate was incorporated in the multilayer system in the desired position and with dose control. Due to the modular nature of click systems, the polymer−drug conjugate could also be incorporated into other click systems. The close control over properties and drug loading, as demonstrated for these stratified biodegradable capsules, makes these systems versatile candidates as drug delivery vehicles.

RESULTS AND DISCUSSION

(PVPON/PGA$_{Alk}$)$_5$ multilayer films were assembled on planar silica substrates. Figure 1A shows the linear increase in layer thickness with the number of deposited layers for buildup at pH 4, as monitored by ellipsometry for films measured in air. At this pH, hydrogen bonds between the carboxylic acid side chains of PGA (pK_a = 4.375)[68] (donor) and PVPON (acceptor) are established, resulting in the formation of multilayer films. The average bilayer thickness under these conditions was calculated as 1.21 ± 0.04 nm. Washing of the
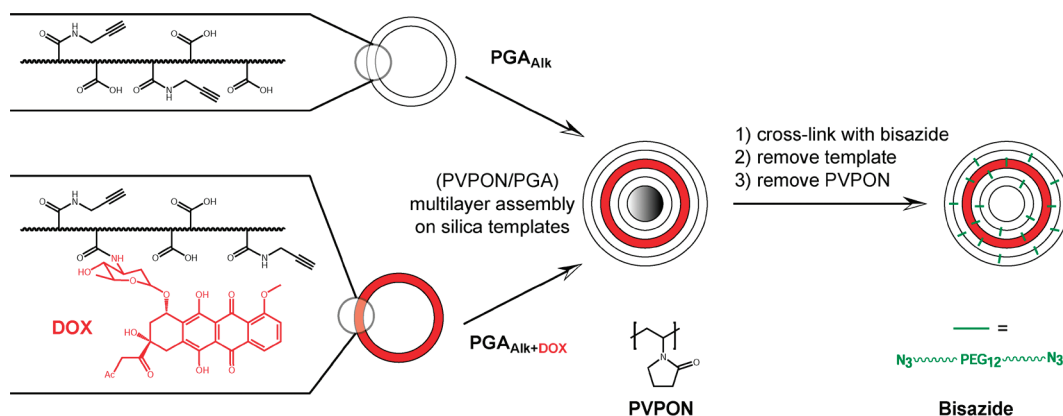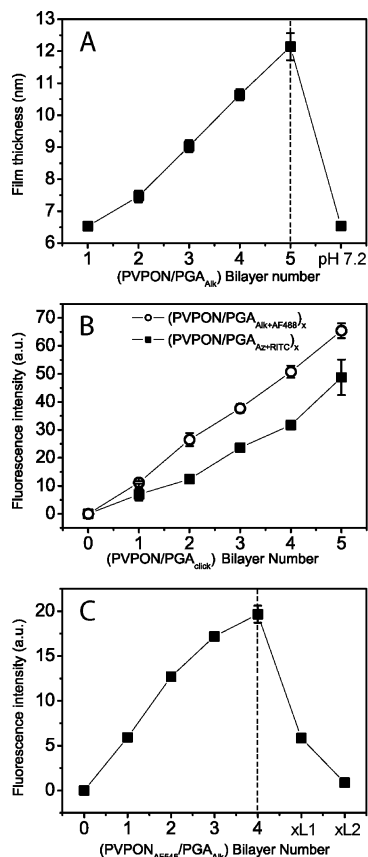
Scheme 1. Modular assembly of PGA$_{Alk}$ (white) click capsules with drug-loaded multilayers. The polymer−drug conjugate (PGA$_{Alk+DOX}$, red) can be incorporated in defined positions and with controlled dose, after which the multilayer films are crosslinked *via* click chemistry using a bisazide crosslinker (green bars).
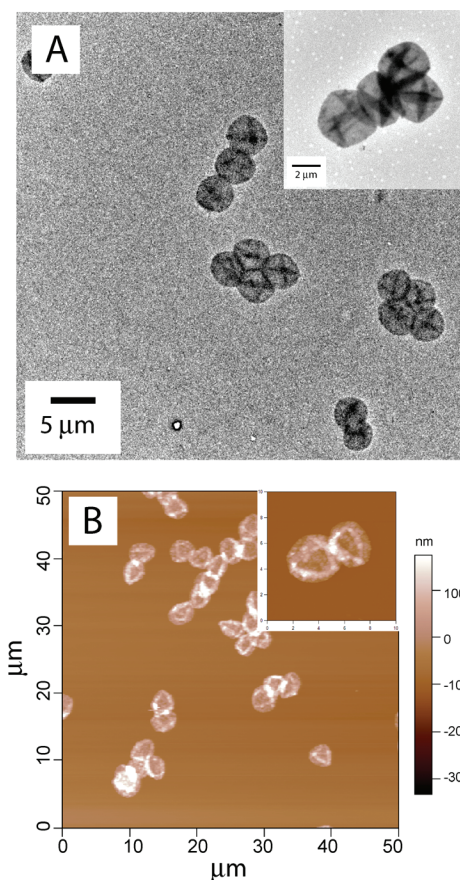
polymer-coated wafer slides with phosphate buffered saline (PBS) resulted in disassembly of the multilayer film, as raising the pH above the pK_a of PGA disrupts the hydrogen bonding interaction between PVPON and PGA$_{Alk}$.

Figure 1. Hydrogen bonding assembly of (PVPON/PGA$_{Alk}$) films in water at pH 4. (A) On planar silica supports, as monitored by ellipsometry for dry films; pH 7.2 refers to the film thickness after washing with PBS. (B) Assembly of (PVPON/PGA$_{Alk+AF488}$)$_5$ and (PVPON/PGA$_{Az+RITC}$)$_5$ multilayer films on 3 μm diameter silica particles, as monitored by flow cytometry. (C) Assembly of (PVPON$_{AF546}$/PGA$_{Alk}$)$_4$ films on 3 μm silica templates, with xL1 = cross-linked core−shell particles washed with PBS, and xL2 = capsules washed with PBS. Error bars, where not visible, are within the size of the symbols.

Fluorescently labeled PGA$_{Alk+AF488}$ or PGA$_{Az+RITC}$ was sequentially deposited with PVPON on 3 μm silica particles in water at pH 4. Linear film growth was observed for both (PVPON/PGA$_{Alk+AF488}$) and (PVPON/PGA$_{Az+RITC}$), as monitored *via* the increase in fluorescence intensity per particle (Figure 1B). PGA$_{Alk}$ was used for all further experiments due to the availability of a broader range of bisazide cross-linkers. Regular film growth was also observed for multilayer films assembled using fluorescently labeled PVPON$_{AF546}$ and unlabeled PGA$_{Alk}$ (Figure 1C). After cross-linking the PGA$_{Alk}$ layers, the core−shell particles were washed with PBS. As hydrogen bonding is not effective at pH 7.2, PVPON$_{AF546}$ diffused out of the PGA$_{Alk}$ multilayers, as evidenced by the decrease in fluorescence intensity, leaving behind a single-component PGA film cross-linked with covalent bonds. Figure 1C suggests that not all PVPON$_{AF546}$ was removed from the multilayers after cross-linking (Figure 1C, xL1). This is probably due to the innermost PVPON$_{AF546}$ layer (=the first layer on the silica particles) not being affected by the disruption of hydrogen bonding upon a change in the solution pH. However, after core removal, the diffusion of PVPON$_{AF546}$ out of the PGA click capsules was observed (Figure 1C, xL2).

The silica core of the core−shell particles was dissolved to yield one-component PGA click capsules. After several washes with water, the isolated capsules were analyzed with TEM (Figure 2A) and AFM (Figure 2B). The capsules obtained were found to collapse and exhibited folds and creases, which are typical for a range of polyelectrolyte capsules.[11,12,26] The close contact of the capsules is due to the drying process required for TEM and AFM analysis (negligible aggregation was observed in solution; see CLSM images in Figure 6). The layer thickness extracted from the AFM height profiles of representative capsules was calculated as 1.9 ± 0.4 nm, which is slightly higher than that obtained from ellipsometry. Such differences in thickness may, in part, be attributed to variations in the silica surface properties for the planar and particle substrates.[26]

Figure 2. (A) TEM and (B) AFM images of cross-linked (PGA$_{Alk}$)$_5$ capsules obtained from 3 μm diameter silica particles. AFM images for scanned areas of 50 × 50 μm² (B) and 10 × 10 μm² (inset).

PGA click capsules obtained from 1, 3, or 5 μm diameter silica templates were stable over a range of pH values (pH 2 and 11) and showed reversible pH-responsive swelling/shrinking behavior over a large number of cycles (Figure 3 and Supporting Information Figure S1), as expected from results obtained previously for conventional (PGA$_{Az}$/PGA$_{Alk}$) click capsules.[11] If exposed to pH 11, the glutamic acid side chains of PGA are deprotonated (negative charge), resulting in electrostatic repulsion between adjoining layers, causing capsule swelling. In contrast, in pH 2 media, the carboxylic acid
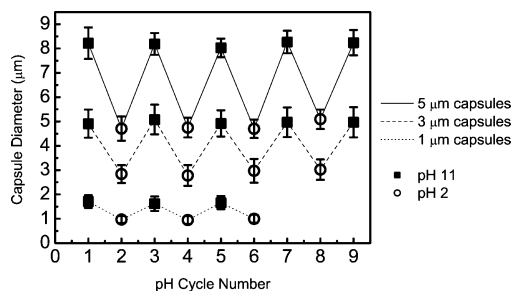
Figure 3. Reversible pH-responsive behavior of (PGA$_{Alk}$)$_5$ capsules obtained from 1, 3, and 5 μm diameter templates. The average capsule diameter after sequential exposure to pH 2 (○) and pH 11 (■) solutions was calculated from 10 differential interference microscopy images.
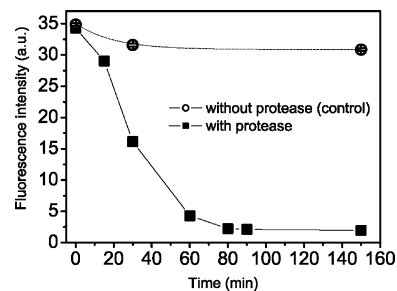

Figure 4. Degradation of cross-linked (PGA$_{Alk+AF488}$)$_6$ films on 3 μm diameter silica particles with 0.1 mg mL^{-1} protease in PBS at 37 °C, as monitored by flow cytometry.

groups are protonated, leading to negligible electrostatic repulsion, and resulting in shrinking of the capsules. Changes in electrostatic interactions induced by pH or ionic strength are well-known to cause capsule swelling and shrinking.[10,69−71] As shown in Figure 3, the capsule size varied by as much as 83% for capsules obtained from 3 μm templates (pH 2, 2.78 ± 0.43 μm; pH 11, 5.08 ± 0.61 μm). Similar swellability was observed for the capsules obtained from 1 and 5 μm templates (80 and 76%, respectively). Compared to the conventional (PGA$_{Az}$/PGA$_{Alk}$) click capsules (28% swelling), the higher swellability found here can be attributed to the different cross-linking density and the additional flexibility provided by the bisazide cross-linker. In the conventional case, PGA$_{Az}$ and PGA$_{Alk}$ are covalently attached directly *via* the triazole linkage, whereas in this study, longer and more flexible cross-linkers were used. A higher swellability achieved by simple variation of the cross-linker length and density is promising with respect to tuning of the pH-responsive shrinking/swelling behavior, which may be used as a triggered loading/release mechanism.

As PGA is a biodegradable polypeptide, the PGA multilayer films should be susceptible to enzymatic degradation. Consequently, the degradability of the cross-linked PGA$_{Alk}$ films was investigated by exposing fluorescently labeled (PVPON/PGA$_{Alk+AF488}$)$_5$ multilayer films to a 0.1 mg mL^{-1} protease solution in PBS at 37 °C (Figure 4). Degradation was complete after approximately 1 h, as monitored by the decrease in fluorescence intensity. A control sample of particles incubated in the absence of protease had stable fluorescence intensity for at least 150 min. Tuning of the cross-linking degree *via* modification of PGA with alkyne groups is expected to influence the degradation kinetics and is promising as a control mechanism for the release of cargo.

We further synthesized a novel polymer−drug conjugate for the controlled assembly and degradation of drug-loaded multilayer click capsules. PGA$_{Alk}$ was modified with the model drug DOX, which is a potent and well-studied DNA intercalating agent. The drug was covalently bound to the reactive carboxylic acid side chains of PGA *via* amide bond formation. The conjuga-
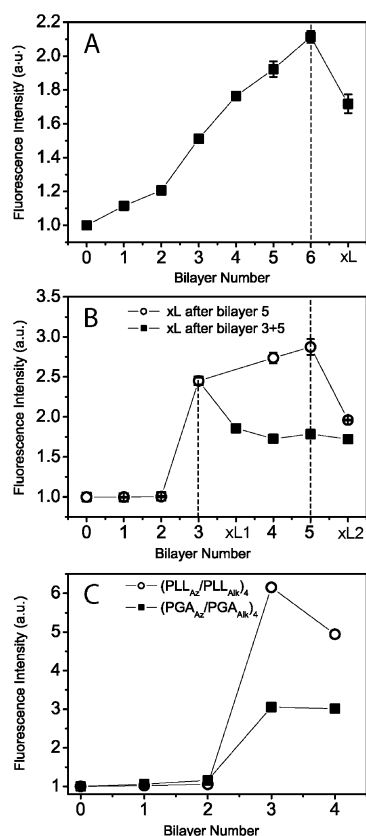
Figure 5. Assembly of DOX-loaded multilayer films on 3 μm diameter silica particles, as monitored by flow cytometry. (A) $(PVPON/PGA_{Alk+DOX})_6$ films; xL refers to cross-linked samples washed with PBS. (B) $(PVPON/PGA_{Alk})_5$ films incorporating $PGA_{Alk+DOX}$ in bilayer 3; xL1 refers to cross-linking (for ■ samples only); xL2 refers to cross-linking of ■ and ○ samples. (C) $(PLL_{Az}/PLL_{Alk})_4$ and $(PGA_{Az}/PGA_{Alk})_4$ multilayer click films. $PGA_{Alk+DOX}$ was incorporated in bilayer 3, substituting for the respective PLL_{Alk} or PGA_{Alk}.

tion significantly reduced the cytotoxicity of DOX and allowed for controlled release of active DOX only after enzymatic degradation of $PGA_{Alk+DOX}$ capsules. A further advantage of the polymer−drug conjugate is that, prior to drug release, the assembly and fate of the capsules can be examined using the inherent fluorescence of DOX. As mentioned earlier, this conjugate not only can be incorporated at defined positions in the multilayer system but also allows for high precision over the drug dose simply by controlling the number of $PGA_{Alk+DOX}$ layers as well as the initial degree of PGA modification with DOX. Furthermore, the polymer−drug conjugate is generally applicable to a variety of click systems due to the modular nature of the assembly.

Multilayer films of PVPON and $PGA_{Alk+DOX}$ were assembled on 3 μm silica particles at pH 4. Due to the fluorescent nature of DOX, the assembly could be monitored *via* the increase in fluorescence per incorporated $PGA_{Alk+DOX}$ layer in a flow cytometry assay. As shown in Figure 5A, film growth is regular for the polymer−drug conjugate. Hence, the additional modification with DOX does not impair the ability of PGA to form hydro-
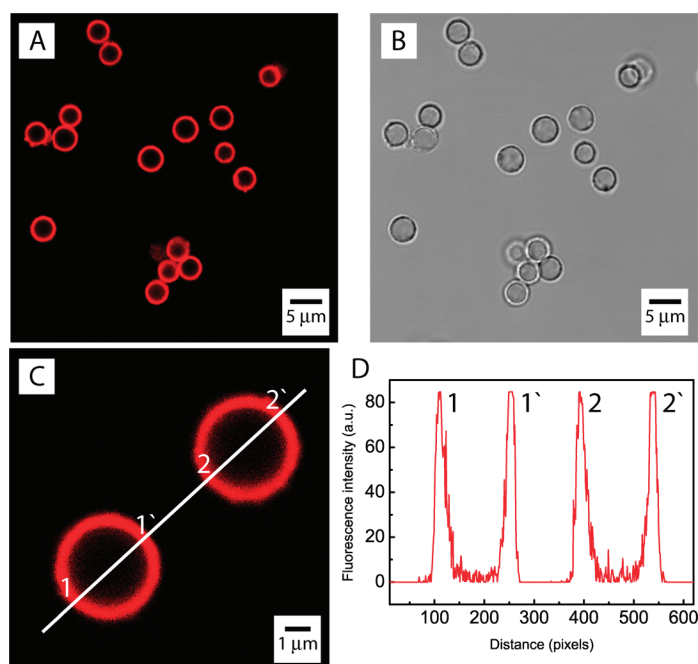

Figure 6. Microscopy images of cross-linked $(PGA_{Alk+DOX})_6$ capsules obtained from 3 μm diameter silica particles. (A,B) CLSM fluorescence and bright-field images. (C,D) Magnified image of two capsules and their corresponding fluorescence profile.

gen bonds with PVPON under these conditions. It was observed that, after cross-linking and washing into PBS, the fluorescence of the core−shell particles decreased, which is probably due to loss of some of the polymer−drug conjugate during washing.

CLSM images of the $(PGA_{Alk+DOX})_6$ capsules reveal a uniform distribution of the polymer−drug conjugate and a regular, spherical shape of the capsules (Figure 6A,B). A profile line drawn across representative capsules shows that DOX is only present in the walls of the capsules and not in the core (Figure 6C,D). Upon exposure to media of different pH, these capsules exhibited the same reversible pH-responsive swellability observed for PGA_{Alk} capsules without DOX (data not shown).

To demonstrate the versatility of the incorporation of polymer−drug conjugates in LbL click capsules, $PGA_{Alk+DOX}$ was assembled at a defined position in the multilayer system. Successful incorporation was evidenced by an increase in fluorescence intensity for the third bilayer (Figure 5B). Upon addition of further $(PVPON/PGA_{Alk})$ bilayers, the fluorescence intensity continued to increase (Figure 5B, ○). This is probably due to rearrangement of the polymer−drug conjugate inside the multilayer system, causing a reduction in the self-quenching of DOX.[67,72] As observed by Hammond *et al.*, the diffusion of polymers inside multilayer systems can be contained by cross-linking.[47,48,73,74] Indeed, the suggested rearrangement could be stopped if the sample was cross-linked directly after DOX incorporation (Figure 5B, ■), and upon the addition of more layers, the fluorescence remained stable after an initial de-
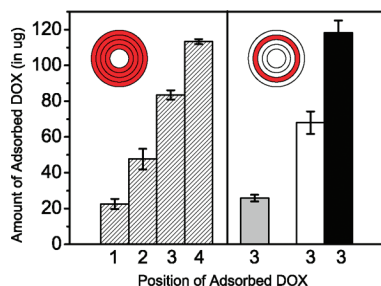
Figure 7. Quantification of the amount of DOX incorporated in the layers of different click systems, as calculated from the supernatant absorbance at $\lambda = 486$ nm using UV−vis and NanoDrop UV−vis spectrophotometry. **Left:** $PGA_{Alk+DOX}$ in every layer for $(PVPON/PGA_{Alk+DOX})_4$ films (hatched). **Right:** $PGA_{Alk+DOX}$ only in bilayer 3 for $(PVPON/PGA_{Alk})_4$ films (gray), $(PGA_{Az}/PGA_{Alk})_4$ films (white), or $(PLL_{Az}/PLL_{Alk})_4$ films (black).

Figure 8. Enzymatic degradation of $(PGA_{Alk+DOX})_6$ capsules obtained from 3 μm diameter silica particles, as monitored by flow cytometry. Degradation with 0.1 mg mL^{-1} protease was carried out in PBS at 37 °C. A control sample of capsules was incubated in the absence of protease.

crease. These experiments indicate that the polymer−drug conjugate may be fixed in a certain layer position by cross-linking of the multilayer system. Control over the cargo position in these stratified systems may result in different release kinetics of the drug from the multilayers and even time-tunable multidose release depending on the number and position of the polymer−drug conjugate layers.

The general applicability of the polymer−drug conjugate was demonstrated by incorporating $PGA_{Alk+DOX}$ into the recently reported (PLL_{Az}/PLL_{Alk}) and (PGA_{Az}/PGA_{Alk}) click films.[11] Again, the polymer−drug conjugate was included in bilayer position 3 in both systems, and the successful incorporation was monitored with flow cytometry (Figure 5C). As this experiment was carried out using the same instrument settings as for the $(PVPON/PGA_{Alk+DOX})$ systems, the increase in fluorescence intensities in bilayer 3 is directly comparable, showing that for the conventional click systems a higher amount of polymer−drug conjugate is incorporated (see also Figure 7). Furthermore, continued layering with (PGA_{Az}/PGA_{Alk}) does not lead to a loss of fluorescence intensity, as the polymer−drug is immediately "fixed" during the assembly. For the (PLL_{Az}/PLL_{Alk}) multilayer films, an even larger increase of fluorescence was observed, which can be explained by the additional electrostatic interaction driving the assembly of the negatively charged polymer−drug conjugate. The subsequent decrease of fluorescence is probably due to removal of noncovalently bound polymer−drug conjugate during the subsequent LbL assembly.

The incorporation of $PGA_{Alk+DOX}$ for all of the above-mentioned experiments was also confirmed independently with UV−vis and NanoDrop UV−vis spectrophotometry to quantify the amount of DOX in the multilayer systems. After deposition of the respective $PGA_{Alk+DOX}$ layers, the supernatant was collected, diluted, and the absorption at $\lambda = 486$ nm was measured. The amount of adsorbed DOX was calculated from a calibration curve for DOX in water. As shown in Figure 7 and supported by the results obtained from flow cytometry experiments, the incorporation of the
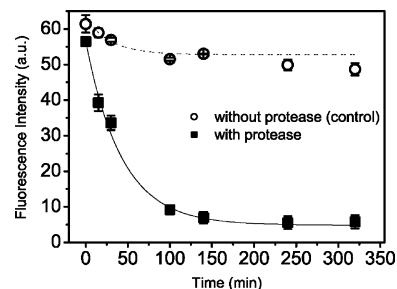
polymer−drug conjugate using LbL assembly follows a linear trend and, hence, allows for precise control over the amount of incorporated drug (hatched series). A similar amount of DOX per layer ($\sim$25 μg) was loaded into the multilayers, even if only one layer of conjugate was asssembled at a defined position (gray). For the conventional (PGA_{Az}/PGA_{Alk}) and (PLL_{Az}/PLL_{Alk}) click systems, higher amounts of drug (75 and 125 μg, respectively) could be loaded due to additional electrostatic interaction with PLL (black) and immediate conjugation of the cargo *via* click chemistry.

DOX-loaded capsules were incubated with protease in PBS at 37 °C, and the progress of PGA degradation was monitored with flow cytometry by measuring the decrease in fluorescence intensity due to loss of the polymer−drug conjugate (Figure 8). Release of DOX from the capsules was complete after $\sim$2 h, which was further evidenced by strong red background fluorescence and the absence of capsules under a fluorescence microscope (Supporting Information Figure S2). From the initial DOX loading (as quantified above), the amount of DOX released per capsule was calculated as approximately 1.28 $\pm$ 0.2 pg. The fluorescence of a control sample of capsules incubated in the absence of protease remained stable for more than 6 h. Control over the degradation profile (*e.g.*, *via* variation of the cross-linking density or layer number) is expected to allow for tailoring of the drug release profile. The remaining carboxylic acid and alkyne groups in the capsule layers and surface may be used for further postfunctionalization, as demonstrated for PLL capsules previously.[11] The ability to load polymer−drug conjugates in defined positions and doses into different click capsules and to subsequently release the drug cargo makes these systems promising candidates for delivery applications.

Polymer solutions of PGA_{Alk} and $PGA_{Alk+DOX}$ and multilayer capsules thereof were also incubated with LIM1899 cells to investigate their effect on cell viability and to examine the toxicity of the polymer−drug conjugate. The MTT assay (Figure 9) showed that, even at high concentrations, the proliferation of cells was not impaired by unmodified PGA or PGA_{Alk} (**T2 + T3**). Importantly, no change in cell proliferation was observed
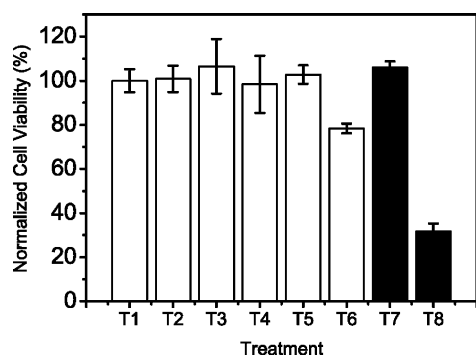
Figure 9. Cell proliferation of LIM1899 cells in the presence of PGA polymer materials (white) and capsules (black) after 48 h of incubation. Cells were: **T1** = untreated; or treated with **T2** = PGA; **T3** = PGA$_{Alk}$; **T4** = PGA$_{Alk+DOX}$; **T5** = protease; **T6** = protease + PGA$_{Alk+DOX}$; **T7** = (PGA$_{Alk}$)$_6$ capsules; **T8** = (PGA$_{Alk+DOX}$)$_6$ capsules. Cells were incubated with capsules at a ratio of 1:24. Data show the mean and standard error of two independent experiments, each performed in triplicate.

after the treatment with PGA$_{Alk+DOX}$ at high concentration (100 µg mL^{-1}, equivalent to 25 µg mL^{-1} of free DOX) (**T4**), in agreement with previous studies on PGA-$_{DOX}$ conjugates.[66,75] It has been reported that a conjugate of Paclitaxel and PGA exhibits better solubility and higher antitumoral activity than free Paclitaxel.[61,62] This apparent difference in cytotoxicity may be explained by the different mechanisms of therapeutic action, as DOX intercalates into DNA in the nucleus, whereas Paclitaxel stabilizes microtubules to interfere with mitotic spindle function in the cytoplasm. When the polymer−drug conjugate was incubated with protease before addition to the cells (**T6**), the cell viability decreased to 78%, presumably due to partially or completely cleaved DOX entering the cells more easily as compared to the nondegraded conjugate. A control sample of protease (at the same concentration used for **T6**) had no negative effect on cell viability (**T5**), confirming that the cytotoxic effect was due to the enzymatic release of DOX.

In contrast, significantly decreased cell viability (32%) and proliferation were observed only after treatment with capsules assembled from PGA$_{Alk+DOX}$ (**T8**), whereas capsules assembled from the unloaded carrier material (PGA$_{Alk}$) proved to have no effect on cell proliferation (**T7**). It is also notable that PGA$_{ALK+DOX}$ capsules exhibited enhanced cytotoxicity compared to the enzymatically digested PGA$_{Alk+Dox}$ conjugate, suggesting that the degradation of the capsules and the cleavage of DOX take place more effectively inside the cells, which may be attributed to the presence of more active or specific enzymes. Furthermore, drug-loaded capsules carry a larger "payload" as compared to the free conjugates and can be fine-tuned to provide desired pharmacokinetic properties with careful control of size and surface chemistry.

To correlate the observed cytotoxicity with cellular uptake and release of DOX, we evaluated the intracellu-
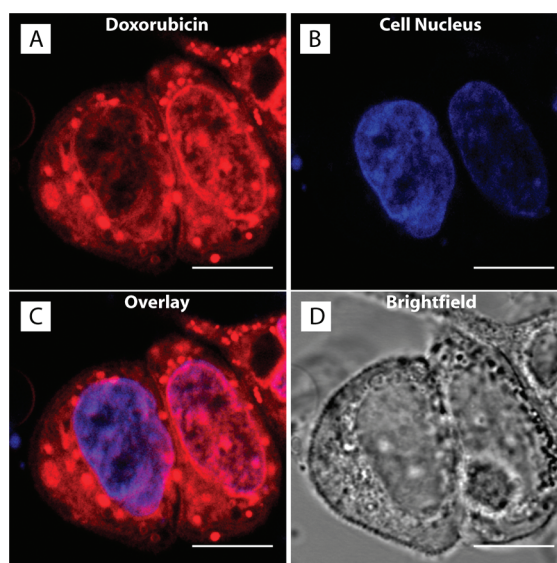
Figure 10. Representative CLSM images of LIM1899 cells treated with (PGA$_{Alk+DOX}$)$_6$ capsules obtained from 3 µm diameter silica particles after 24 h incubation. (A) Red fluorescence corresponds to DOX, (B) Nuclear DNA was stained blue with Hoechst 33342. (C) Overlay image showing colocalization of DOX and nuclei. (D) Brightfield image. All scale bars are 10 µm.

lar distribution of DOX delivered by PGA$_{Alk+DOX}$ capsules and free polymer by incubating them with LIM1899 cells for 24 h. As shown in Figure 10 for cells incubated with capsules, DOX-associated fluorescence was present in the cytoplasm, largely concentrated in vesicles at the perinuclear region, and a significant proportion of DOX was localized in the nuclei of the LIM1899 cells. This suggests that some free DOX had been released from the capsules and further translocated to the nucleus by previously reported mechanisms.[76] These involve binding of DOX to cytoplasmic proteasome, formation of a proteasome−DOX complex, and subsequent accumulation in the nucleus by a nuclear pore-mediated mechanism. In contrast, significantly weaker DOX-associated fluorescence was observed if cells were incubated with equivalent amounts of the free polymer−drug conjugate (Supporting Information Figure S3). More importantly, no DOX was further translocated to the nucleus after treatment with the polymer−drug conjugate. The images also support the data obtained in the MTT assay because DOX can be located in the nucleus only after treatment with DOX-loaded capsules, resulting in significantly decreased viability as compared to the free polymer−drug conjugate. The different uptake behavior and subsequent effect of DOX on cell viability for either the capsule or free polymer−drug conjugates highlights the importance of the LbL approach to produce drug-loaded capsules with engineered properties. The nontoxicity of the carrier system and the controlled release of DOX from drug-loaded capsules after enzymatic degradation exclusively inside the cells make this polymer−drug conjugate a highly interesting ma-

terial for drug delivery applications. The high level of control over drug dose and position afforded by the modular LbL assembly approach with regard to tuning of the release kinetics and killing efficiency is promising.

CONCLUSIONS

In summary, we have presented a versatile approach for the assembly of biodegradable, covalently stabilized drug-loaded capsules (PGA$_{Alk+DOX}$) with control over drug dose and layer position. Regular film growth on planar (for PGA$_{Alk}$) and particle substrates was observed. In the case of particles, cross-linking of the layers and core removal yielded stable PGA$_{Alk}$ capsules. The single-component capsules exhibited reversible, pH-responsive properties (up to 83% swelling). Due to the modularity of the click LbL approach, the polymer−drug conjugate was incorporated into the multilayer systems with control over drug position and dose (on average 25 μg of DOX per layer for hydrogen bonding assembly). DOX-loaded capsules were enzymatically degraded, resulting in release of active DOX over ~2 h. A decrease in cell viability (32% in comparison to untreated cells) and colocalization of DOX with the nuclei of LIM1899 cells were only observed if the polymer−drug conjugate was delivered as a "click capsule", highlighting the importance of the presented approach to produce drug-loaded biodegradable capsules. The conjugate was also incorporated into other click systems, showing its general applicability. The optional incorporation of new modules (similar polymer−drug conjugates or PEGylated PGA) makes this approach promising for the synthesis of multifunctional, drug-loaded, and degradable carrier systems.

EXPERIMENTAL SECTION

Materials. Poly(L-glutamic acid, sodium salt) (PGA, M_w = 50 000−70 000 Da) and poly(N-vinyl pyrrolidone) (PVPON, M_w = 55 000 Da) were purchased from Sigma-Aldrich. Doxorubicin hydrochloride (DOX, purity 99+%) was purchased from OChem Inc. (Des Plaines, IL). Nonporous colloidal silica particles (5 wt % suspensions, average diameter 5.35 ± 0.25, 3.25 ± 0.18, and 1.11 ± 0.05 μm) were obtained from Microparticles GmbH (Berlin, Germany). Protease (from Streptomyces griseus, 4.6 units/mg solid) was obtained from Sigma-Aldrich. Gibco phosphate buffered saline (PBS) at pH 7.2 was used as received. Unless specified otherwise, all other chemicals were purchased from Sigma-Aldrich and used as received.

The pH of solutions was measured with a Mettler-Toledo MP220 pH meter. High-purity water with a resistivity greater than 18 MΩ·cm was obtained from an in-line Millipore RiOs/Origin water purification system. Silicon wafers were obtained from MMRC Pty Ltd. (Melbourne, Australia). Cleaning of silicon wafers for ellipsometry and atomic force microscopy (AFM) experiments was performed by submerging slides in Piranha solution (70/30 v/v sulfuric acid/hydrogen peroxide) for 20 min and rinsing thoroughly with water. [*Caution! Piranha solution is highly corrosive. Extreme care should be taken when handling Piranha solution and only small quantities should be prepared.*] This process was repeated, and the slides were sonicated in 50 v/v isopropanol/water for 20 min. Afterward, the slides were heated to 60 °C in RCA solution (5:1:1 water/hydrogen peroxide/ammonia solution) for 20 min. Finally, substrates were washed with water and dried under a stream of nitrogen.

Polymer Synthesis. Details of the synthesis of PGA with alkyne or azide functionality (referred to as PGA$_{Alk}$ and PGA$_{Az}$, respectively) and their fluorescently labeled counterparts (Alexa Fluor 488 for PGA$_{Alk+AF488}$ and rhodamine B isothiocyanate for PGA$_{Az+RITC}$) can be found in our previous publication.[11] The modification of PGA with DOX, fluorescent dyes, or click groups is indicated by subscripts. PGA with 20% click functionalization (alkyne or azide) was used throughout this study. The polymer−drug conjugate (PGA$_{Alk+DOX}$) was synthesized by dissolving 40 mg (0.18 mmol GA, 1 equiv) of PGA$_{Alk}$ in 10 mL of water. One hundred milligrams (0.36 mmol, 2 equiv.) of 4-(4,6-dimethoxy-1,3,5-triazin-2-yl)-4-methylmorpholinium chloride (DMTMM) and 20 mg (0.04 mmol, 0.2 equiv.) of doxorubicin hydrochloride were then added, and the clear, red solution was stirred at room temperature overnight. The product was dialyzed extensively and further purified using a Sephadex column to remove nonbound doxorubicin. The solution was lyophilized to give 50 mg (0.16 mmol, 88%) of a red powder. NMR analysis showed that 10% of the glutamic acid side chains were modified with doxorubicin: ^{1}H NMR (400 MHz, D$_2$O) δ$_H$ 1.17−1.27 (dd, DOX-CH$_3$), 1.84−2.14 and 2.14−2.40 (m, CH$_α$(CH$_2$)$_2$CONH polymer and DOX), 2.42−2.58 (m, DOX), 2.63 (br s, CCH click group), 3.60−3.63, 3.67−3.72, 3.73−3.8 (m, DOX), 3.85 (br s, DOX-OMe), 3.93−3.99 (br s, CONHCH$_2$ click group), 4.00−4.05 (br s, DOX), 4.24−4.44 (br s, CH$_α$ polymer), 5.34−5.37 (m, DOX), 7.11−7.37 (m, DOX aromatic), 7.47−7.59 (m, DOX aromatic) ppm.

Cross-Linker Synthesis. Details of the synthesis of the nonreducible cross-linker (bisazido dodecaethylene glycol, herein referred to as bisazide) can be found elsewhere.[39]

Multilayer Assembly on Planar Supports. For (PVPON/PGA$_{Alk}$) multilayer assembly, wafer slides were sequentially immersed into solutions containing 1 mg mL^{-1} of PVPON or PGA$_{Alk}$ at pH 4. A period of 20 min was allowed for the deposition of each layer, after which the slides were rinsed with water at pH 4 three times for 1 min and dried with nitrogen. As a control experiment, one slide was washed with PBS after deposition of four bilayers at pH 4.

Multilayer Assembly on Colloidal Supports. One hundred microliters of the particle stock solution was washed with water at pH 4. Then, 400 μL of the PVPON solution was added to the pellet, and adsorption was allowed to proceed for 20 min with constant shaking of the mixture. Afterward, the particles were isolated by centrifugation (1300g for 1 min), and the supernatant was removed. In a washing step, 400 μL of pH 4 water was added. The particles were then redispersed, centrifuged again, and the washing procedure was repeated twice. For adsorption of the next layer, 400 μL of the PGA$_{Alk}$ solution was added, followed by the same washing protocol. PGA multilayer films were prepared by repeating this process until the desired number of layers was obtained. Afterward, the PGA$_{Alk}$ layers were cross-linked overnight by adding a mixture of 300 μL of bisazide,[39] 100 μL of sodium ascorbate (4.4 mg mL^{-1}), and 100 μL of copper sulfate (1.75 mg mL^{-1}). The PVPON was subsequently removed by washing the core−shell particles with PBS three times.

For the assembly of drug-loaded multilayer click films, the PGA$_{Alk}$ solution was substituted with a 2 mg mL^{-1} of PGA$_{Alk+DOX}$ solution adjusted to pH 4. Hollow capsules were formed by dissolving the core using hydrogen fluoride (HF) buffered to pH 5 with ammonium fluoride.[77] Three washing steps (4500g for 5 min, replacing the supernatant with fresh water) were applied to remove the HF and isolate the capsules for analysis.

Degradation of PGA$_{Alk}$ Multilayer Films. Core−shell particles with cross-linked PGA$_{Alk}$ or PGA$_{Alk+DOX}$ multilayer capsules were washed into PBS and counted on the flow cytometer. Then, 5 × 10^5 particles were incubated with 0.1 mg mL^{-1} protease solution in PBS at 37 °C. A control sample of particles was incubated in PBS only. Aliquots were taken after the indicated periods of time, and the fluorescence was monitored with flow

cytometry. The degradation of the PGA$_{Alk}$ click film was also monitored by fluorescence microscopy.

MTT Assay. The interference of PGA$_{Alk}$ and PGA$_{Alk+DOX}$ capsules with cell proliferation was assessed in an MTT assay as described previously.[78] The human colon cancer cell line LIM1899 was plated at 1×10^4 cells per well into 96-well plates.[79] After 20 h attachment, cells were exposed to 100 μg mL^{-1} of PGA$_{Alk}$ polymer, 100 μg mL^{-1} of PGA$_{Alk+DOX}$ polymer, or capsules composed of either polymer (6 PGA layers, obtained from 3 μm silica templates) at a concentration of 1200 capsules μL^{-1} (equivalent to a capsule/cell ratio of 24:1). After treatment for 48 h (at 37 °C, 5% CO$_2$), the medium was replaced with 200 μL of MTT solution (Sigma, 0.5 g L^{-1}), and cells were incubated for a further 2 h. The resulting blue formazan was solubilized in 150 μL of acidified isopropanol (0.04 M HCl), and the absorbance at 560 nm was measured with a plate reader (MultiskanAscent, Thermo Scientific). The MTT reduction of untreated cells was set as 100%, and that of treated cells was expressed as a percentage of untreated cells. Each experiment was performed in triplicate.

Intracellular Release of DOX from PGA$_{Alk+DOX}$ Capsules. LIM1899 cells were plated at 8×10^4 cells/well into 8-well Lab-Tek I chambered coverglass slides (Thermo Fisher Scientific, Rochester) and allowed to adhere overnight. Cells were then incubated with PGA$_{Alk+DOX}$ capsules at a concentration of 1200 capsules μL^{-1} for 24 h (37 °C, 5% CO$_2$), followed by three washes with PBS. Cells were then fixed with 4% paraformaldehyde for 20 min at room temperature, and nuclei were counterstained with the blue dye Hoechst 33342 (2 μg mL^{-1} in PBS) for 20 min at room temperature.

Analytical Methods. Film thicknesses were determined with a Jobin Yvon UVISEL spectroscopic ellipsometer. Typical measurements were carried out between 400 and 800 nm with a 2 nm increment. Layer thicknesses (measured in air) were extracted with the integrated software by fitting the experimental data with a classical wavelength dispersion model. Flow cytometry measurements were carried out on a Partec CyFlow Space (Partec GmbH, Germany) flow cytometer at an excitation wavelength of 488 nm. Data were analyzed according to the procedure outlined previously.[80] Differential interference contrast (DIC) and fluorescence images were taken on an inverted Olympus IX71 microscope equipped with a DIC slider (U-DICT, Olympus) with a 60× objective lens (Olympus UPFL20/0.5 NA, W.D. 1.6). A CCD camera was mounted on the left-hand port of the microscope. A tungsten lamp was used for DIC images. Fluorescence images were illuminated with an Hg arc lamp, using a UF1032 filter cube. Confocal microscopy images were obtained using a Leica TCS-SP2 confocal laser scanning microscope (CLSM). For AFM and transmission electron microscopy (TEM) measurements, 1 μL of a concentrated capsule solution was placed on a clean silicon wafer slide (or TEM grid) and allowed to dry. AFM scans were carried out with an MFP-3D Asylum Research instrument in AC mode using ultrasharp SiN gold-coated cantilevers (NT-MDT). TEM analysis was carried out with a Philips CM 120 microscope operated at 120 kV. The amount of adsorbed doxorubicin was quantified via absorbance readings at $\lambda = 486$ nm using a NanoDrop 1000 spectrophotometer (Thermo Scientific, Australia) and an Agilent 8453 UV−visible spectrophotometer (Agilent Technologies, CA).

Supporting Information Available: Optical microscopy images of the responsive swelling behavior of (PGA$_{Alk}$)$_5$ capsules (PGA$_{Alk+DOX}$)$_6$ capsule enzymatic degradation, and PGA$_{Alk+DOX}$ free polymer uptake. This material is available free of charge via the Internet at http://pubs.acs.org.

REFERENCES AND NOTES

1. Kiick, K. L. Polymer Therapeutics. *Science* **2007**, *317*, 1182–1183.
2. De Geest, B. G.; De Koker, S.; Sukhorukov, G. B.; Kreft, O.; Parak, W. J.; Skirtach, A. G.; Demeester, J.; De Smedt, S. C.; Hennink, W. E. Polyelectrolyte Microcapsules for Biomedical Applications. *Soft Matter* **2009**, *5*, 282–291.
3. Peyratout, C. S.; Dahne, L. Tailor-Made Polyelectrolyte Microcapsules: From Multilayers to Smart Containers. *Angew. Chem., Int. Ed.* **2004**, *43*, 3762–3783.
4. Ariga, K.; Hill, J. P.; Ji, Q. M. Layer-by-Layer Assembly as a Versatile Bottom-Up Nanofabrication Technique for Exploratory Research and Realistic Application. *Phys. Chem. Chem. Phys.* **2007**, *9*, 2319–2340.
5. Stadler, B.; Chandrawati, R.; Price, A. D.; Chong, S. F.; Breheney, K.; Postma, A.; Connal, L. A.; Zelikin, A. N.; Caruso, F. A Microreactor with Thousands of Subcompartments: Enzyme-Loaded Liposomes within Polymer Capsules. *Angew. Chem., Int. Ed.* **2009**, *48*, 4359–4362.
6. Price, A. D.; Zelikin, A. N.; Wang, Y.; Caruso, F. Triggered Enzymatic Degradation of DNA within Selectively Permeable Polymer Capsule Microreactors. *Angew. Chem., Int. Ed.* **2009**, *48*, 329–332.
7. Decher, G.; Hong, J. D. Buildup of Ultrathin Multilayer Films by a Self-Assembly Process 0.2. Consecutive Adsorption of Anionic and Cationic Bipolar Amphiphiles and Polyelectrolytes on Charged Surfaces. *Ber. Bunsen-Ges. Phys. Chem.* **1991**, *95*, 1430–1434.
8. Stockton, W. B.; Cheung, J. H.; Rubner, M. F. Molecular-Level Processing of Conjugated Polymers 0.3. Layer-by-Layer Manipulation of Polyaniline via Electrostatic Interactions. *Macromolecules* **1997**, *30*, 2712–2716.
9. Johnston, A. P. R.; Read, E. S.; Caruso, F. DNA Multilayer Films on Planar and Colloidal Supports: Sequential Assembly of Like-Charged Polyelectrolytes. *Nano Lett.* **2005**, *5*, 953–956.
10. Such, G. K.; Quinn, J. F.; Quinn, A.; Tjipto, E.; Caruso, F. Assembly of Ultrathin Polymer Multilayer Films by Click Chemistry. *J. Am. Chem. Soc.* **2006**, *128*, 9318–9319.
11. Ochs, C. J.; Such, G. K.; Stadler, B.; Caruso, F. Low-Fouling, Biofunctionalized, and Biodegradable Click Capsules. *Biomacromolecules* **2008**, *9*, 3389–3396.
12. Kinnane, C. R.; Wark, K.; Such, G. K.; Johnston, A. P. R.; Caruso, F. Peptide-Functionalized, Low-Biofouling Click Multilayers for Promoting Cell Adhesion and Growth. *Small* **2009**, *5*, 444–448.
13. De Geest, B. G.; Van Camp, W.; Du Prez, F. E.; De Smedt, S. C.; Demeester, J.; Hennink, W. E. Biodegradable Microcapsules Designed via 'Click' Chemistry. *Chem. Commun.* **2008**, 190–192.
14. Kozlovskaya, V.; Kharlampieva, E.; Mansfield, M. L.; Sukhishvili, S. A. Poly(methacrylic acid) Hydrogel Films and Capsules: Response to pH and Ionic Strength, and Encapsulation of Macromolecules. *Chem. Mater.* **2006**, *18*, 328–336.
15. Kozlovskaya, V.; Shamaev, A.; Sukhishvili, S. A. Tuning Swelling, pH and Permeability of Hydrogel Multilayer Capsules. *Soft Matter* **2008**, *4*, 1499–1507.
16. Kohli, P.; Blanchard, G. J. Design and Demonstration of Hybrid Multilayer Structures: Layer-by-Layer Mixed Covalent and Ionic Interlayer Linking Chemistry. *Langmuir* **2000**, *16*, 8518–8524.
17. Serizawa, T.; Nanameki, K.; Yamamoto, K.; Akashi, M. Thermoresponsive Ultrathin Hydrogels Prepared by Sequential Chemical Reactions. *Macromolecules* **2002**, *35*, 2184–2189.
18. Picart, C.; Schneider, A.; Etienne, O.; Mutterer, J.; Schaaf, P.; Egles, C.; Jessel, N.; Voegel, J. C. Controlled Degradability of Polysaccharide Multilayer Films In Vitro and In Vivo. *Adv. Funct. Mater.* **2005**, *15*, 1771–1780.
19. Tong, W. J.; Gao, C. Y.; Moehwald, H. pH-Responsive Protein Microcapsules Fabricated via Glutaraldehyde Mediated Covalent Layer-by-Layer Assembly. *Colloid Polym. Sci.* **2008**, *286*, 1103–1109.
20. Lee, D.; Rubner, M. F.; Cohen, R. E. Formation of Nanoparticle-Loaded Microcapsules Based on Hydrogen-Bonded Multilayers. *Chem. Mater.* **2005**, *17*, 1099–1105.
21. Zhang, H.; Yang, B.; Wang, R. B.; Zhang, G.; Hou, X. L.; Wu,

L. X. Fabrication of a Covalently Attached Self-Assembly Multilayer Film Based on CdTe Nanoparticles. *J. Colloid Interface Sci.* **2002**, *247*, 361–365.

22. Rydzek, G.; Thomann, J.; Ben Ameur, N.; Jierry, L. ; Msini, P.; Ponche, A.; Contal, C.; El Haitami, A.; Voegel, J.; Senger, B.; Schaaf, P.; Frisch, B.; Boulmedais, F. Polymer Multilayer Films Obtained by Electrochemically Catalyzed Click Chemistry. *Langmuir* **2010**, *26*, 2816−2824.

23. Tong, W. J.; Gao, C. Y. Stable Microcapsules Assembled Stepwise from Weak Polyelectrolytes Followed by Thermal Crosslinking. *Polym. Adv. Technol.* **2005**, *16*, 827–833.

24. Iha, R. K.; Wooley, K. L.; Nystrom, A. M.; Burke, D. J.; Kade, M. J.; Hawker, C. J. Applications of Orthogonal "Click" Chemistries in the Synthesis of Functional Soft Materials. *Chem. Rev.* **2009**, *109*, 5620–5686.

25. Vestberg, R.; Malkoch, M.; Kade, M.; Wu, P.; Fokin, V. V.; Sharpless, K. B.; Drockenmuller, E.; Hawker, C. J. Role of Architecture and Molecular Weight in the Formation of Tailor-Made Ultrathin Multilayers Using Dendritic Macromolecules and Click Chemistry. *J. Polym. Sci. Polym. Chem.* **2007**, *45*, 2835–2846.

26. Such, G. K.; Tjipto, E.; Postma, A.; Johnston, A. P. R.; Caruso, F. Ultrathin, Responsive Polymer Click Capsules. *Nano Lett.* **2007**, *7*, 1706–1710.

27. Lutz, J. F. 1,3-Dipolar Cycloadditions of Azides and Alkynes: A Universal Ligation Tool in Polymer and Materials Science. *Angew. Chem., Int. Ed.* **2007**, *46*, 1018–1025.

28. Bock, V. D.; Hiemstra, H.; van Maarseveen, J. H. Cu-I-Catalyzed Alkyne-Azide "Click" Cycloadditions from a Mechanistic and Synthetic Perspective. *Eur. J. Org. Chem.* **2006**, 51–68.

29. Peschke, B.; Bak, S. Controlled Coupling of Peptides at Their C-Termini. *Peptides* **2009**, *30*, 689–698.

30. Thonon, D.; Kech, C.; Paris, J.; Lemaire, C.; Luxen, A. New Strategy for the Preparation of Clickable Peptides and Labeling with 1-(Azidomethyl)-4-F-18-fluorobenzene for PET. *Bioconjugate Chem.* **2009**, *20*, 817–823.

31. Zelikin, A. N.; Becker, A. L.; Johnston, A. P. R.; Wark, K. L.; Turatti, F.; Caruso, F. A General Approach for DNA Encapsulation in Degradable Polymer Microcapsules. *ACS Nano* **2007**, *1*, 63–69.

32. Chong, S. F.; Sexton, A.; De Rose, R.; Kent, S. J.; Zelikin, A. N.; Caruso, F. A Paradigm for Peptide Vaccine Delivery Using Viral Epitopes Encapsulated in Degradable Polymer Hydrogel Capsules. *Biomaterials* **2009**, *30*, 5178–5186.

33. Zelikin, A. N.; Li, Q.; Caruso, F. Disulfide-Stabilized Poly(methacrylic acid) Capsules: Formation, Cross-Linking, and Degradation Behavior. *Chem. Mater.* **2008**, *20*, 2655–2661.

34. De Geest, B. G.; Vandenbroucke, R. E.; Guenther, A. M.; Sukhorukov, G. B.; Hennink, W. E.; Sanders, N. N.; Demeester, J.; De Smedt, S. C. Intracellularly Degradable Polyelectrolyte Microcapsules. *Adv. Mater.* **2006**, *18*, 1005–1009.

35. Itoh, Y.; Matsusaki, M.; Kida, T.; Akashi, M. Enzyme-Responsive Release of Encapsulated Proteins from Biodegradable Hollow Capsules. *Biomacromolecules* **2006**, *7*, 2715–2718.

36. Borodina, T.; Markvicheva, E.; Kunizhev, S.; Moehwald, H.; Sukhorukov, G. B.; Kreft, O. Controlled Release of DNA from Self-Degrading Microcapsules. *Macromol. Rapid Commun.* **2007**, *28*, 1894–1899.

37. Wattendorf, U.; Kreft, O.; Textor, M.; Sukhorukov, G. B.; Merkle, H. P. Stable Stealth Function for Hollow Polyelectrolyte Microcapsules through a Poly(ethylene glycol) Grafted Polyelectrolyte Adlayer. *Biomacromolecules* **2008**, *9*, 100–108.

38. Heuberger, R.; Sukhorukov, G.; Voros, J.; Textor, M.; Mohwald, H. Biofunctional Polyelectrolyte Multilayers and Microcapsules: Control of Non-specific and Bio-specific Protein Adsorption. *Adv. Funct. Mater.* **2005**, *15*, 357–366.

39. Kinnane, C. R.; Such, G. K.; Antequera-Garcia, G.; Yan, Y.; Dodds, S. J.; Liz-Marzan, L.; Caruso, F. Low-Fouling Poly(*N*-vinyl pyrrolidone) Capsules with Engineered Degradable Properties. *Biomacromolecules* **2009**, *10*, 2839−2846.

40. Lasser, A. The Mononuclear Phagocytic System—A Review. *Hum. Pathol.* **1983**, *14*, 108–126.

41. Cortez, C.; Tomaskovic-Crook, E.; Johnston, A. P. R.; Radt, B.; Cody, S. H.; Scott, A. M.; Nice, E. C.; Heath, J. K.; Caruso, F. Targeting and Uptake of Multilayered Particles to Colorectal Cancer Cells. *Adv. Mater.* **2006**, *18*, 1998–2003.

42. Angelatos, A. S.; Radt, B.; Caruso, F. Light-Responsive Polyelectrolyte/Gold Nanoparticle Microcapsules. *J. Phys. Chem. B* **2005**, *109*, 3071–3076.

43. Jung, J.; Lee, I. H.; Lee, E.; Park, J.; Jon, S. pH-Sensitive Polymer Nanospheres for Use as a Potential Drug Delivery Vehicle. *Biomacromolecules* **2007**, *8*, 3401–3407.

44. Sukhorukov, G. B.; Brumen, M.; Donath, E.; Mohwald, H. Hollow Polyelectrolyte Shells: Exclusion of Polymers and Donnan Equilibrium. *J. Phys. Chem. B* **1999**, *103*, 6434–6440.

45. Schneider, A.; Vodouhe, C.; Richert, L.; Francius, G.; Le Guen, E.; Schaaf, P.; Voegel, J. C.; Frisch, B.; Picart, C. Multifunctional Polyelectrolyte Multilayer Films: Combining Mechanical Resistance, Biodegradability, and Bioactivity. *Biomacromolecules* **2007**, *8*, 139–145.

46. Hosta-Rigau, L.; Stadler, B.; Yan, Y.; Nice, E. C.; Heath, J. K.; Albericio, F.; Caruso, F. Capsosomes with Multilayered Subcompartments: Assembly and Loading with Hydrophobic Cargo. *Adv. Funct. Mater.* **2010**, *20*, 59.

47. Wood, K. C.; Chuang, H. F.; Batten, R. D.; Lynn, D. M.; Hammond, P. T. Controlling Interlayer Diffusion to Achieve Sustained, Multiagent Delivery from Layer-by-Layer Thin Films. *Proc. Natl. Acad. Sci. U.S.A.* **2006**, *103*, 10207–10212.

48. Kim, B.-S.; Smith, R. C.; Poon, Z.; Hammond, P. T. MAD (Multiagent Delivery) Nanolayer: Delivering Multiple Therapeutics from Hierarchically Assembled Surface Coatings. *Langmuir* **2009**, *25*, 14086−14092.

49. Khopade, A. J.; Caruso, F. Stepwise Self-Assembled Poly(amidoamine) Dendrimer and Poly(styrenesulfonate) Microcapsules as Sustained Delivery Vehicles. *Biomacromolecules* **2002**, *3*, 1154–1162.

50. Tao, X.; Chen, H.; Sun, X. J.; Chen, H. F.; Roa, W. H. Formulation and Cytotoxicity of Doxorubicin Loaded in Self-Assembled Bio-polyelectrolyte Microshells. *Int. J. Pharm.* **2007**, *336*, 376–381.

51. Sivakumar, S.; Bansal, V.; Cortez, C.; Chong, S. F.; Zelikin, A. N.; Caruso, F. Degradable, Surfactant-Free, Monodisperse Polymer-Encapsulated Emulsions as Anticancer Drug Carriers. *Adv. Mater.* **2009**, *21*, 1820–1824.

52. Fox, M. E.; Szoka, F. C.; Frechet, J. M. J. Soluble Polymer Carriers for the Treatment of Cancer: The Importance of Molecular Architecture. *Acc. Chem. Res.* **2009**, *42*, 1141–1151.

53. Gillies, E. R.; Goodwin, A. P.; Frechet, J. M. J. Acetals as pH-Sensitive Linkages for Drug Delivery. *Bioconjugate Chem.* **2004**, *15*, 1254–1263.

54. Guillaudeu, S. J.; Fox, M. E.; Haidar, Y. M.; Dy, E. E.; Szoka, F. C.; Frechet, J. M. J. PEGylated Dendrimers with Core Functionality for Biological Applications. *Bioconjugate Chem.* **2008**, *19*, 461–469.

55. Schneider, G. F.; Subr, V.; Ulbrich, K.; Decher, G. Multifunctional Cytotoxic Stealth Nanoparticles. A Model Approach with Potential for Cancer Therapy. *Nano Lett.* **2009**, *9*, 636–642.

56. Jourdainne, L.; Arntz, Y.; Senger, B.; Debry, C.; Voegel, J. C.; Schaaf, P.; Lavalle, P. Multiple Strata of Exponentially Growing Polyelectrolyte Multilayer Films. *Macromolecules* **2007**, *40*, 316–321.

57. Tryoen-Toth, P.; Vautier, D.; Haikel, Y.; Voegel, J. C.; Schaaf, P.; Chluba, J.; Ogier, J. Viability, Adhesion, and Bone Phenotype of Osteoblast-like Cells on Polyelectrolyte Multilayer Films. *J. Biomed. Mater. Res.* **2002**, *60*, 657–667.

58. Chiu, H. C.; Kopeckova, P.; Deshmane, S. S.; Kopecek, J. Lysosomal Degradability of Poly(α-amino acids). *J. Biomed. Mater. Res.* **1997**, *34*, 381–392.

59. Nair, L. S.; Laurencin, C. T. Biodegradable Polymers as Biomaterials. *Prog. Polym. Sci.* **2007**, *32*, 762–798.

60. Li, C. Poly(L-glutamic acid)—Anticancer Drug Conjugates. *Adv. Drug Delivery Rev.* **2002**, *54*, 695–713.

61. Li, C.; Yu, D. F.; Newman, R. A.; Cabral, F.; Stephens, L. C.; Hunter, N.; Milas, L.; Wallace, S. Complete Regression of Well-Established Tumors Using a Novel Water-Soluble Poly(L-glutamic acid) Paclitaxel Conjugate. *Cancer Res.* **1998**, *58*, 2404–2409.

62. Shaffer, S. A.; Baker Lee, C.; Kumar, A.; Singer, J. W. Proteolysis of Xyotax by Lysosomal Cathepsin B; Metabolic Profiling in Tumor Cells Using LC-MS. *Eur. J. Cancer* **2002**, *38*, 428.

63. Wen, X. X.; Jackson, E. F.; Price, R. E.; Kim, E. E.; Wu, Q. P.; Wallace, S.; Charnsangavej, C.; Gelovani, J. G.; Li, C. Synthesis and Characterization of Poly(L-glutamic acid) Gadolinium Chelate: A New Biodegradable MRI Contrast Agent. *Bioconjugate Chem.* **2004**, *15*, 1408–1415.

64. Richert, L.; Arntz, Y.; Schaaf, P.; Voegel, J. C.; Picart, C. pH Dependent Growth Of Poly(L-lysine)/poly(L-glutamic) Acid Multilayer Films and Their Cell Adhesion Properties. *Surf. Sci.* **2004**, *570*, 13–29.

65. Hubsch, E.; Fleith, G.; Fatisson, J.; Labbe, P.; Voegel, J. C.; Schaaf, P.; Ball, V. Multivalent Ion/Polyelectrolyte Exchange Processes in Exponentially Growing Multilayers. *Langmuir* **2005**, *21*, 3664–3669.

66. Wang, Y.; Bansal, V.; Zelikin, A. N.; Caruso, F. Templated Synthesis of Single-Component Polymer Capsules and Their Application in Drug Delivery. *Nano Lett.* **2008**, *8*, 1741–1745.

67. Yap, H. P.; Johnston, A. P. R.; Such, G. K.; Yan, Y.; Caruso, F. Click-Engineered, Bioresponsive, Drug-Loaded PEG Spheres. *Adv. Mater.* **2009**, *21*, 4348–4352.

68. Nilsson, S.; Zhang, W. Helix-Coil Transition of a Titrating Polyelectrolyte Analyzed within the Poisson−Boltzmann Cell Model—Effects of pH and Salt Concentration. *Macromolecules* **1990**, *23*, 5234–5239.

69. Dejugnat, C.; Sukhorukov, G. B. pH-Responsive Properties of Hollow Polyelectrolyte Microcapsules Templated on Various Cores. *Langmuir* **2004**, *20*, 7265–7269.

70. Biesheuvel, P. M.; Mauser, T.; Sukhorukov, G. B.; Mohwald, H. Micromechanical Theory for pH-Dependent Polyelectrolyte Multilayer Capsule Swelling. *Macromolecules* **2006**, *39*, 8480–8486.

71. Mauser, T.; Dejugnat, C.; Sukhorukov, G. B. Balance of Hydrophobic and Electrostatic Forces in the pH Response of Weak Polyelectrolyte Capsules. *J. Phys. Chem. B* **2006**, *110*, 20246–20253.

72. Leroux, J. C.; Roux, E.; Le Garrec, D.; Hong, K. L.; Drummond, D. C. N-Isopropylacrylamide Copolymers for the Preparation of pH-Sensitive Liposomes and Polymeric Micelles. *J. Controlled Release* **2001**, *72*, 71–84.

73. Zacharia, N. S.; DeLongchamp, D. M.; Modestino, M.; Hammond, P. T. Controlling Diffusion and Exchange in Layer-by-Layer Assemblies. *Macromolecules* **2007**, *40*, 1598–1603.

74. Yoo, P. J.; Zacharia, N. S.; Doh, J.; Nam, K. T.; Belcher, A. M.; Hammond, P. T. Controlling Surface Mobility in Interdiffusing Polyelectrolyte Multilayers. *ACS Nano* **2008**, *2*, 561–571.

75. Vega, J.; Ke, S.; Fan, Z.; Wallace, S.; Charsangavej, C.; Li, C. Targeting Doxorubicin to Epidermal Growth Factor Receptors by Site-Specific Conjugation of C225 to Poly(L-glutamic acid) through a Polyethylene Glycol Spacer. *Pharm. Res.* **2003**, *20*, 826–832.

76. Kiyomiya, K.; Matsuo, S.; Kurebe, M. Mechanism of Specific Nuclear Transport of Adriamycin: The Mode of Nuclear Translocation of Adriamycin−Proteasome Complex. *Cancer Res.* **2001**, *61*, 2467–2471.

77. Wang, Y.; Caruso, F. Template Synthesis of Stimuli-Responsive Nanoporous Polymer-Based Spheres *via* Sequential Assembly. *Chem. Mater.* **2006**, *18*, 4089–4100.

78. Postma, A.; Yan, Y.; Wang, Y.; Zelikin, A. N.; Tjipto, E.; Caruso, F. Self-Polymerization of Dopamine as a Versatile and Robust Technique to Prepare Polymer Capsules. *Chem. Mater.* **2009**, *21*, 3042–3044.

79. Andrew, S. M.; Teh, J. G.; Johnstone, R. W.; Russell, S. M.; Whitehead, R. H.; McKenzie, I. F. C.; Pietersz, G. A. Tumor-Localization by Combinations of Monoclonal-Antibodies in a New Human Colon-Carcinoma Cell-Line (Lim1899). *Cancer Res.* **1990**, *50*, 5225–5230.

80. Johnston, A. P. R.; Zelikin, A. N.; Lee, L.; Caruso, F. Approaches to Quantifying and Visualizing Polyelectrolyte Multilayer Film Formation on Particles. *Anal. Chem.* **2006**, *78*, 5913–5919.

ARTICLE